*Applied Science and Engineering Progress, Vol. 20, No. 3, 2027, 8314*

Research Article

# Hygrothermal Durability of CNT-Modified Recycled Carbon Fiber/Epoxy Laminates: Moisture Diffusion and Mechanical Property Retention

Anchal Sharma* and Sunny Zafar
Composite Design and Manufacturing Research Group, School of Mechanical and Materials Engineering, Indian Institute of Technology Mandi, Kamand, Mandi-175075, India

* Corresponding author. E-mail: rudrakshanchal@gmail.com DOI: 10.14416/j.asep.2026.09.006
Received: 11 June 2026; Revised: 4 August 2026; Accepted: 7 August 2026; Published online: 9 September 2026


**Abstract**
The growing use of carbon fiber-reinforced polymer composites has increased the need for effective recycling and high-value reuse of recovered carbon fibers. This study investigates the influence of direct carbon nanotube (CNT) growth on the seawater hygrothermal durability of recycled carbon fiber/epoxy laminates. Carbon fibers were recovered through microwave-assisted chemical recycling, modified by microwave-assisted carbon nanotube growth, and remanufactured using vacuum-assisted resin infusion followed by microwave curing. The novelty of the present work lies in integrating microwave-assisted carbon fiber recovery, direct CNT growth, VARIMC remanufacturing, and seawater hygrothermal durability assessment within a unified recycling-to-reuse framework. The unmodified and carbon nanotube-modified laminates were exposed to accelerated seawater ageing, followed by moisture diffusion, tensile, impact, and fracture-surface analyses. Carbon nanotube modification reduced the equilibrium moisture uptake from 1.20 to 0.72 mass% and decreased the diffusion coefficient from $3.09 \times 10^{-13}$ to $2.31 \times 10^{-13}$ m²/s. After ageing, the tensile strength decreased from 412.3 to 336.6 MPa for the unmodified laminate and from 509.7 to 460.8 MPa for the modified laminate, corresponding to strength retentions of 81.64% and 90.41%, respectively. The impact strength retention also increased from 42.83% to 69.78% after carbon nanotube modification. Fracture-surface observations indicated improved fiber–matrix adhesion, crack bridging, and greater energy dissipation in the modified laminates. These results demonstrate that carbon nanotube modification can improve the moisture resistance and mechanical durability of recycled carbon fiber composites for marine structures, offshore components, wind energy systems, and lightweight automotive applications.

**Keywords**: Carbon nanotube modification, Fractography, Mechanical durability, Microwave-assisted chemical recycling, Moisture diffusion, Recycled carbon-fiber composites, Seawater hygrothermal ageing

## 1 Introduction

Carbon fiber reinforced polymer (CFRP) composites are widely used in aerospace, marine, automotive, and structural applications because of their high strength-to-weight ratio and good stiffness [1], [2]. The increasing use of CFRP has also generated large amounts of manufacturing scrap and end-of-life composite waste [3], [4]. Manufacturing scrap and end-of-life CFRP parts are difficult to reuse because the thermoset matrix cannot be remelted or reshaped [5], [6]. Recovery and reuse of carbon fibers from CFRP waste have therefore become important for reducing material cost, energy demand, and environmental impact [7]. There are many ways to recycle CFRP waste, such as mechanical, chemical, and thermal methods [8], [9]. Mechanical recycling is easy, but it usually produces short fibers and makes the reinforcement less effective [5], [10]. Chemical recycling can recover cleaner fibers, but it usually needs strong solvents, high temperatures, high pressures, and liquid waste treatment after the process [11]. In thermal recycling and pyrolysis processes, the polymer matrix can be removed effectively, but the recovered fibers may lose quality due to char formation and surface damage [5]. Because of these limitations, microwave-assisted recycling is being used as a faster and more controlled method for recovering fibers [9], [12].

Microwave causes rapid, uniform and volumetric heating, potentially expediting matrix degradation and decreasing processing time [13]-[15]. Deng *et al.,* stated

Applied Science and Engineering Progress, Vol. 20, No. 3, 2027, 8314

that microwave thermolysis increased the carbon fiber recovery ratio and decreased the reaction time in comparison to traditional thermolysis [9]. Lester *et al.,* additionally demonstrated that microwave heating can eliminate the polymer matrix and retrieve clean carbon fibers suitable for reuse in high-grade applications [12]. These studies suggest that microwave processing can be a viable method for the recovery of carbon fibers from CFRP waste. These recovered recycled carbon fibers can be used again for the fabrication of composites, but their surface condition is a major concern [5], [16]. Residual matrix and surface irregularities can reduce the bonding between the recovered fibers and the fresh epoxy matrix [17]. This issue becomes more critical under seawater or humid service conditions. Moisture can move into the laminate through the epoxy matrix, fiber/matrix interface, microvoids, and pre-existing damaged regions [17], [18]. This leads to matrix plasticization, swelling, interfacial debonding, and microcrack formation. These damage processes reduce stress transfer between fiber and matrix and lower the tensile and impact performance of the laminate.

Carbon nanotube (CNT) modification is a useful approach to improve the fiber/matrix interphase in recycled CFRP laminates [19], [20]. Das *et al.,* demonstrated that MWCNT modification strengthens fiber–matrix stress transfer and improves mechanical performance in fiber-reinforced epoxy composites, directly supporting the interfacial enhancement observed in the present CNT-reinforced carbon fiber polymer composite system [21]. CNTs grown on the recycled fiber surface can increase surface roughness and improve mechanical interlocking with the epoxy matrix [22], [23]. A CNT-rich interphase can also increase the moisture diffusion path and reduce easy transport routes for seawater [24]. Under mechanical loading, this interphase can promote crack deflection, crack bridging, matrix shear, and fiber pull-out resistance [25]. These mechanisms are important for improving tensile-property retention and impact energy absorption after hygrothermal ageing. The motivation for this work arises from the need to improve the structural reuse of recycled carbon fibers, whose surface damage and weakened fiber-matrix interaction can limit composite durability, particularly under humid and marine conditions. Direct carbon nanotube growth offers a promising route to strengthen the recycled fiber-epoxy interphase, restrict moisture transport and improve mechanical-property retention after hygrothermal ageing.

In the present study, carbon fibers were recovered from laboratory-controlled CFRP laminates and modified by CNT growth on the recycled fiber surface. Unmodified recycled carbon fiber reinforced polymer (rCFRP) and (laminate manufactured using CNT-rCF) CNT-rCFRP laminates were fabricated by vacuum-assisted resin infusion microwave curing (VARIMC) process and exposed to seawater hygrothermal ageing. The moisture uptake behaviour was analysed to compare seawater transport in both laminates. Tensile and Izod impact tests were then performed to evaluate post-ageing mechanical performance. SEM fractography was used to identify the fracture mechanisms responsible for the observed tensile and impact behaviour. The study aims to clarify how CNT modification affects moisture resistance, interfacial stability, and damage tolerance in recycled CFRP laminates.

## 2 Experimental Details

### 2.1 *Materials*

The composite laminates investigated in this study were based on woven bi-directional carbon-fiber reinforcement and an epoxy thermoset matrix. A woven carbon-fiber (CF) mat of 200 GSM with 0°/90° fiber architecture, procured from Bhor Chemicals and Plastics Pvt. Ltd., was used as the reinforcing material. Lapox ARL-135LV epoxy resin and Lapox AH-337 hardener, supplied by Lopax Pvt. Ltd., were used as the matrix system for composite fabrication. The control composite was a laboratory-made CFRP laminate made by hand lay-up method that was used as the recycling feedstock. It was developed to support the development and assessment of the microwave-assisted recycling approach. It was manufactured under controlled laboratory conditions using the same bi-directional carbon-fiber reinforcement and epoxy matrix system. The laminate had no previous service exposure, environmental ageing, repair history, or prior mechanical loading and was not obtained from an end-of-life component. Using a controlled laboratory-made composite reduced the influence of unknown service conditions and pre-existing damage on the recycling and remanufacturing results.

For the recycling process, extra-pure hydrogen peroxide ($H_2O_2$, 30% w/v) and acetic acid ($CH_3COOH$, 99.5% purity) were procured from Loba Chemie Pvt. Ltd. These served as the chemical reagents. Ferrocene powder, with an average particle size of approximately 20-25 μm and supplied by Loba Chemie, India, was

used as the catalyst precursor for the growth of CNT on the surface of the recycled carbon fiber. Toluene with a purity of 99.5% was employed as the solvent medium to prepare a 0.5 M ferrocene solution for CNT deposition.

### 2.2 *Recycling of CFRP composite*

The eight-ply laboratory-fabricated control CFRP laminate was used as the recycling feedstock. The schematic representation of the recycling route is shown in Figure 1. The CFRP composite laminate of dimensions 280 mm × 280 mm × 4 mm was first immersed in a 50 vol.% $CH_3COOH/H_2O_2$ solution for 30 min. This treatment caused swelling of the composite laminate. The swollen CFRP laminate was then irradiated at 720 W in a 2.45 GHz microwave applicator for 180 s in steps. The stepped cycle consisted of continuous microwave heating for 120 s, followed by a no-irradiation period of 15 min. This cooling interval allowed the onset of self-separation of the recycled carbon fibers from the degraded matrix. The laminate was then reheated for an additional 60 s to complete the decomposition of the epoxy matrix.

Microwave irradiation accelerated the reaction between $CH_3COOH$ and $H_2O_2$, leading to the formation of peracetic acid (PAA). The generated PAA acted as a strong oxidizing agent and disrupted the amine-cured epoxy network, thereby releasing recycled carbon fibers with minimal epoxy residue on the surface. After reaction completion, the recovered fibers were cleaned with acetone and dried at 60 ºC for 2 h. Ansari *et al.,* [13] investigated carbon fibers recovered under the same optimised MACR conditions and reported 99.10% epoxy degradation with only 1.8 wt.% residual mass loss by TGA. The recovered fibers retained approximately 91.8% of the virgin-fiber tensile strength and 94.6% of the tensile modulus, while the interfacial shear strength increased from 40.62 to 52.40 MPa. These findings confirm that the MACR process effectively removed the epoxy matrix while preserving sufficient fiber integrity for composite remanufacturing. Further details of this MACR process and suitability of the process can be found elsewhere [13], [26].

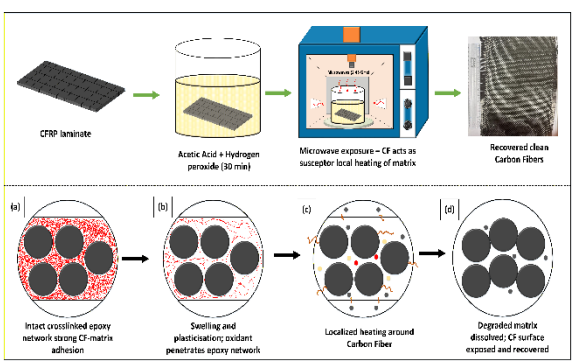


**Figure 1:** MACR of CFRP and the associated microstructural mechanism leading to recovery of clean carbon fibers.

### 2.3 *CNT growth on recycled carbon fibers*

In the second step, the surface of the recycled carbon fibers was modified by growing CNTs on the recovered fiber surface. As shown in Figure 2, the recycled carbon-fiber mat was first dipped in a 0.5 M ferrocene solution for 20 min. Ferrocene acted as the iron catalyst precursor and carbon source, while toluene with a dielectric constant of 2.38 served as the microwave absorber liquid. Before microwave irradiation, a partial vacuum of 0.05 MPa was established inside the microwave cavity to reduce oxidation at elevated temperature and to limit contamination from gaseous products released during ferrocene decomposition. The ferrocene-treated recycled carbon fiber mat was then placed inside the microwave cavity and irradiated at 720 W for 30 s using stepped microwave irradiation. The stepped cycle consisted of 25 s of continuous irradiation, followed by a 15 s pause, and then an additional 5 s of irradiation [23].

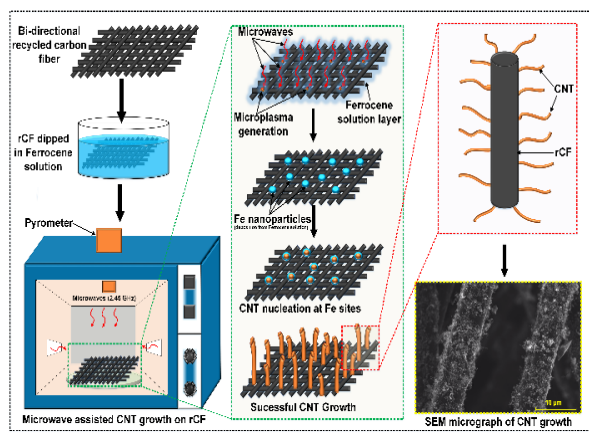


**Figure 2**: Microwave-assisted CNT growth.

During microwave exposure, the conductive carbon fibers and the surrounding toluene absorbed electromagnetic energy, causing a rapid increase in the local temperature. After a critical temperature was reached, dielectric breakdown of toluene produced localized sparks and microplasma near the carbon-fiber surface. In the first stage, these microplasma regions provided sufficient energy for the decomposition of ferrocene. In the second stage, ferrocene decomposed to form iron nanoparticles together with gaseous carbon-containing species, including methane and cyclopentadiene, and hydrogen. The iron nanoparticles deposited on the recycled carbon-fiber surface and acted as catalytic nucleation sites for CNT growth.

In the final stage, carbon species generated from the decomposition of ferrocene and toluene were adsorbed onto the iron nanoparticles. The carbon subsequently dissolved into or diffused across the catalyst particles and precipitated to form graphitic tubular structures. Continuous microwave heating supplied additional carbon species and maintained the catalyst activity, resulting in the progressive outward growth of CNTs from the recycled carbon-fiber surface.

Using a Mettler Toledo analytical balance, mass measurements showed an average increase of 0.80 ± 0.10 mg after CNT development, which corresponds to an apparent CNT deposition of 0.0113 ± 0.0019 weight percent on the surface of recycled carbon fiber. CNT-modified recycled carbon fibers produced under identical processing conditions were previously characterised by Ansari *et al.,* using SEM, Raman spectroscopy, XPS, contact-angle, and AFM analyses. The results confirmed CNT formation and improved surface roughness and wettability, supporting better bonding with the epoxy matrix [13], [23]. SEM showed dense, uniformly distributed hair-like CNTs on the recycled fiber surface. Raman analysis confirmed CNT formation through the D + D′ and G′ bands and a decrease in the $I_D/I_G$ ratio from 1.70 to 0.80. XPS showed increased graphitic character, while the contact angle decreased from 51° to 19° and surface roughness increased from 1.80 to 2.45 nm, confirming improved wettability and surface modification after CNT growth. The resulting CNT-grown recycled carbon fiber (CNT-rCF) was used as the modified reinforcement for composite fabrication.

### 2.4 *Manufacturing of composites*

The laminates were manufactured using the VARIMC process, as shown in Figure 3. In this method, 8 layers of recycled carbon fiber or CNT-modified recycled carbon fiber (CNT-rCF) mats were placed inside a Teflon mold and covered with a vacuum bagging arrangement. Vacuum was created using a vacuum pump, and after ensuring a vacuum level of up to 0.1 MPa, the epoxy resin was infused into the layered fiber mats. A resin-to-hardener ratio of 100:32 was used. After complete resin infusion, the mould was placed in the microwave applicator and cured at 180 W for 8 min [13]. Following microwave exposure, the laminates were maintained under vacuum and cooled naturally to room temperature before demoulding. The suitability of this low-power curing condition is supported by Kumar and Zafar, who reported a DSC-derived degree of cure of 96.3% for carbon-fiber/epoxy laminates processed by VARIMC at 180 W, owing to relatively uniform heating and extensive epoxy crosslinking [14]. Following remanufacturing, the final in-plane dimensions of the rCFRP and CNT-rCFRP laminates were 250 × 250 mm². A total of 2 laminates per material/formulation were manufactured. The average laminate thickness was 2.25 ± 0.34 mm, determined from 5 measurements/specimens. The mechanical-test specimens were cut directly from the remanufactured laminates using grinder.

### 2.5 *Hygrothermal Ageing Set-up*

For the hygrothermal ageing process, a simplified artificial seawater solution containing 3.5 wt.% laboratory-grade NaCl in deionised water was used, while moisture-conditioning measurements were performed in accordance with ASTM D5229/D5229M. The solution pH was maintained within the range of 7.5-8.4, with $Na^+$ and $Cl^-$ as the principal dissolved ions.

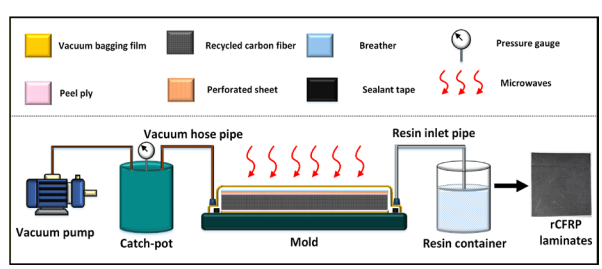


**Figure 3**: VARIMC setup used to manufacture the recycled CFRP laminates.

The ageing bath was maintained at 75 °C using an electric heating coil for 75 days. A temperature data logger was installed to continuously monitor the bath temperature. To ensure uniform temperature distribution and avoid thermal gradients within the chamber, a circulating pump was used to keep the seawater in continuous motion. The ageing solution was not replaced during the exposure period, and the chamber was kept covered to minimize evaporation.

Before conditioning, the specimens were oven-dried at 70 °C for 48 h to remove residual moisture, cooled to room temperature and weighed to obtain their initial dry mass. The prepared composite specimens were then placed on a dedicated sample holder at the bottom of the chamber to ensure complete and uniform immersion during ageing, as shown in Figure 4. Moisture uptake was recorded at regular intervals until the specimens reached saturation. The initial moisture-diffusion behaviour was evaluated from the linear region of the normalized moisture uptake, $M_t/M_\infty$, plotted against the square root of immersion time. The data recorded during the initial 0-8 day period were used for linear regression and calculation of the apparent diffusion coefficient. The complete 75-day uptake response was additionally examined using a dual-Fickian model containing fast and slow diffusion contributions. After the mass gain became nearly constant, the aged specimens were taken out of the seawater bath and tested to evaluate the retention of tensile and impact properties after hygrothermal exposure.

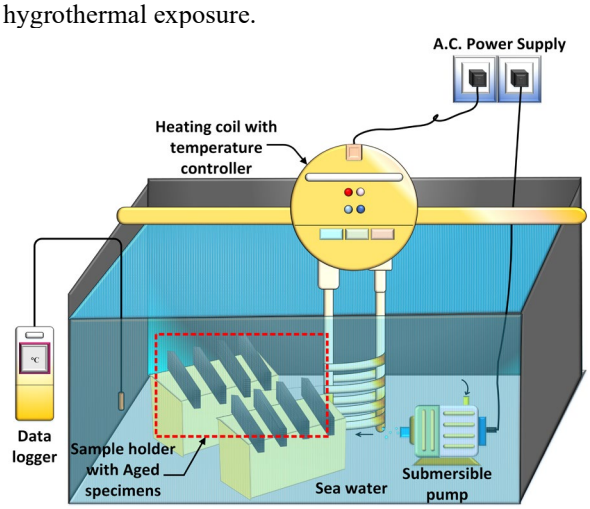


**Figure 4**: Hygrothermal ageing setup.

## 2.6 *Tensile characterization*

The tensile properties of both unaged and seawater-aged rCFRP and CNT-rCFRP laminates were measured using a 250 kN universal testing machine (Instron 8802). The tests were performed at room temperature in accordance with ASTM D3039/D3039M. Rectangular specimens of 250 mm × 25 mm × 2.25 mm were prepared from each laminate. A crosshead speed of 2 mm/min was used. Five specimens were tested for each condition, and the average values were reported.

The tensile response was used to calculate the ultimate tensile strength and tensile modulus. Tensile stress was calculated using:

$$\sigma = \frac{F}{b \times t} \quad (1)$$

where σ is the tensile stress, F is the applied load, b is the specimen width, and t is the specimen thickness. The tensile modulus was obtained from the slope of the initial linear region of the stress-strain curve. Five specimens were tested for each material and ageing condition, and the average values were reported together with the standard deviation. The tensile strength and tensile modulus of the aged specimens were compared with the corresponding unaged values to determine property retention after seawater hygrothermal exposure.

## 2.7 *Impact characterization*

The impact strength of the unaged and seawater-aged rCFRP and CNT-rCFRP laminates was measured using an IC 256 computerized Izod/Charpy impact tester. The test was performed in Izod mode according to ASTM D256. Specimens of 63.5 mm × 12.7 mm × 2.25 mm were prepared from each material and ageing condition. A pendulum hammer with an impact energy of 5.42 J was used for testing. The absorbed energy was recorded during impact and converted into impact strength using the fractured cross-sectional area of the specimen. Five specimens were tested for each material and ageing condition, and the average impact strength was reported together with the standard deviation.

Applied Science and Engineering Progress, Vol. 20, No. 3, 2027, 8314

## 3. Results and Discussion

### *3.1 Moisture uptake behavior of the composites*

Figure 5 shows the moisture uptake behaviour of the rCFRP and CNT-rCFRP laminates during seawater hygrothermal ageing. The mass gain in both laminates increased sharply during the early immersion period and then slowed as the specimen moved towards saturation. The moisture uptake at any time, $M_t$, was calculated using:

$$M_t = \frac{m_t - m_0}{m_0} \times 100 \quad (2)$$

where $m_t$ is the mass at time $t$, and $m_0$ is the initial dry mass of the specimen.

The rCFRP laminate absorbed 1.20 wt.% of moisture, while the CNT-rCFRP laminate absorbed a lower value of 0.72 wt.%. This behavior suggested that CNT modification reduced moisture absorption by approximately 40%. The lower absorption value suggests that the CNT-rich interphase made it difficult for seawater to migrate over interfacial gaps and matrix defects by making the diffusion path tortuous.

Both laminates showed a rapid increase in moisture uptake during the initial immersion period, followed by a gradual reduction in the absorption rate as saturation was approached. The lower equilibrium uptake of CNT-rCFRP indicates improved resistance to seawater penetration.

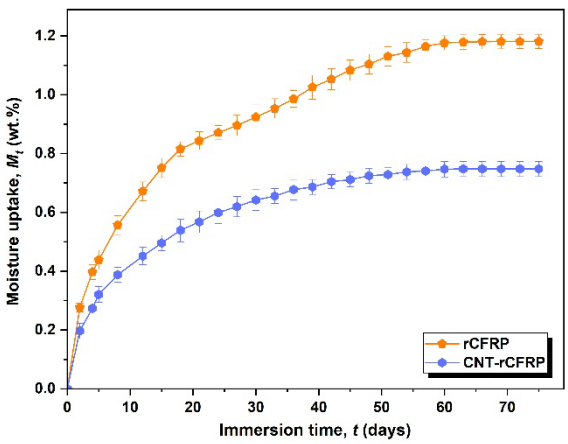


**Figure 5**: Experimental moisture uptake of rCFRP and CNT-rCFRP laminates during 75 days of seawater hygrothermal ageing.

To compare the diffusion behaviour of the two laminates in Figure 6, the moisture-uptake data were normalized using the following equation:

$$M_t^n = \frac{M_t}{M_\infty} \quad (3)$$

where $M_t^n$ is the normalized moisture uptake and $M_\infty$ is the experimentally determined equilibrium moisture uptake.

The initial 0-8 day region showed an approximately linear relationship between $M_t/M_\infty$ and $t_{1/2}$. Linear regression gave $R^2$ values of 0.9999 for rCFRP and 0.9984 for CNT-rCFRP, confirming that the early moisture-uptake response was predominantly Fickian.

The apparent diffusion coefficient (D) was measured from the linear region of the absorption curve using:

$$D = \pi \left(\frac{h}{4M_\infty}\right)^2 \left(\frac{M_b - M_a}{\sqrt{t_b} - \sqrt{t_a}}\right)^2 \quad (4)$$

where $h$ is the specimen thickness, $M_\infty$ is the amount of moisture it can hold at equilibrium, and $M_a$ and $M_b$ are the amounts of moisture it holds at periods $t_a$ and $t_b$, respectively. The specimen thickness *(h)* used in the calculation was $2.25\times10^{-3}$ m, and immersion time was converted into seconds to obtain D in $m^2/s$.

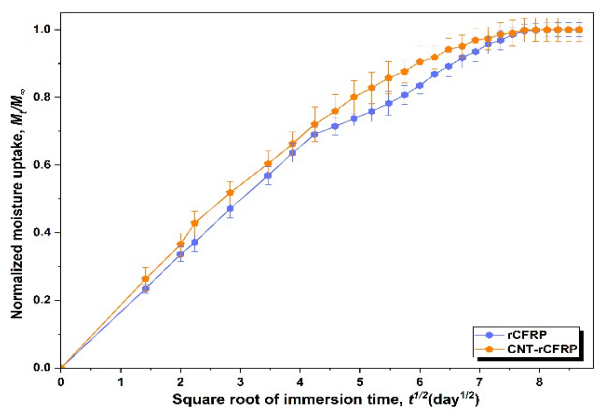


**Figure 6**: Normalized moisture uptake, $M_t/M_\infty$, against the square root of immersion time for rCFRP and CNT-rCFRP laminates.

The calculated diffusion coefficient for the rCFRP laminate was $3.09\times10^{-13}$ m²/s, whereas the CNT-rCFRP laminate showed a lower value of $2.31\times10^{-13}$ m²/s. This represents an approximately 25% reduction in the apparent diffusion coefficient. The reduced diffusion coefficient confirms that moisture transport occurred more slowly in the CNT-modified laminate.

At longer immersion times, both uptake curves gradually departed from the initial linear $M_t/M_\infty$ and $t_{1/2}$ relationship. Therefore, the complete 75-day moisture-uptake response was additionally analysed using a dual-Fickian model:

$$M_t = M_1F(D_1,t) + M_2F(D_2,t) \quad (5)$$

where the Fickian contribution $F(D_i,t)$ is expressed as:

$$F(D_i,t) = 1 - \frac{8}{\pi^2}\sum_{n=0}^{\infty}\frac{1}{(2n+1)^2}\exp\left[-\frac{(2n+1)^2\pi^2 D_i t}{h^2}\right] \quad (6)$$

where, $M_1$ and $M_2$ represent the moisture contributions associated with the faster and slower transport processes, respectively, while $D_1$ and $D_2$ are the corresponding diffusion coefficients.

As shown in Figure 7, the dual-Fickian model achieved $R^2$ values of 0.9976 for rCFRP and 0.9995 for CNT-rCFRP, indicating close agreement with the complete experimental datasets.

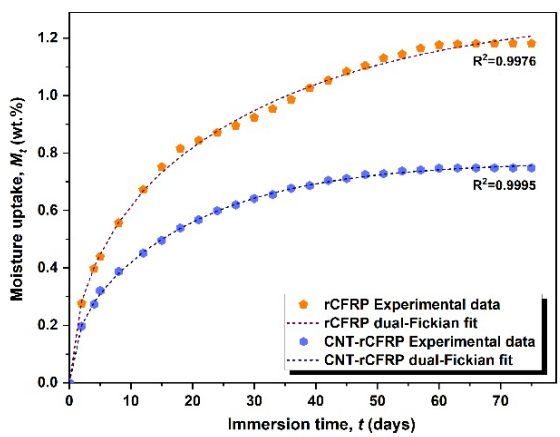


**Figure 7**: Comparison of experimental moisture-uptake data with dual-Fickian model predictions for rCFRP and CNT-rCFRP laminates.

The faster contribution may be associated with initial moisture penetration through readily accessible matrix, microvoid and interfacial pathways, whereas the slower contribution represents delayed transport through the epoxy network and less-accessible internal regions. These contributions provide a phenomenological description of the overall uptake response.

The improved moisture resistance of the CNT-rCFRP laminate can be attributed to the formation of a CNT-rich interphase around the recycled carbon fibers. The presence of CNTs likely increased the tortuosity of the diffusion path, thereby making seawater transport through the laminate more difficult. In addition, CNTs may have improved fiber/matrix interfacial bonding and reduced the availability of microvoids, interfacial gaps, and capillary pathways that normally assist moisture penetration. As a result, both the equilibrium uptake and the diffusion rate were reduced in the CNT-rCFRP laminate.

In contrast, the higher moisture uptake and diffusion coefficient of the rCFRP laminate, as summarized in Table 1, suggest easier seawater transport through the polymer matrix and fiber/matrix interface. This behavior could be caused by weak interfacial regions, residual defects, and local pathways formed during recycling and fabrication of laminates. These pathways can accelerate moisture ingress, leading to matrix softening, interfacial weakening, and gradual damage during prolonged hygrothermal ageing.

**Table 1**: Equilibrium moisture uptake and diffusion coefficient of aged rCFRP and CNT-rCFRP laminates.

| Material | Equilibrium uptake (wt.%) | Diffusion coefficient, D (m²/s) |
|---|---|---|
| rCFRP laminate | 1.20 | $3.09 \times 10^{-13}$ |
| CNT-rCFRP laminate | 0.72 | $2.31 \times 10^{-13}$ |

### *3.2 Tensile properties of the composites before and after hygrothermal ageing*

The tensile strength and tensile modulus of the rCFRP and CNT-rCFRP laminates before and after seawater hygrothermal ageing are presented in Figures 8 and 9. Before ageing, the tensile strengths of rCFRP and CNT-rCFRP were 412.3 and 509.7 MPa, respectively.

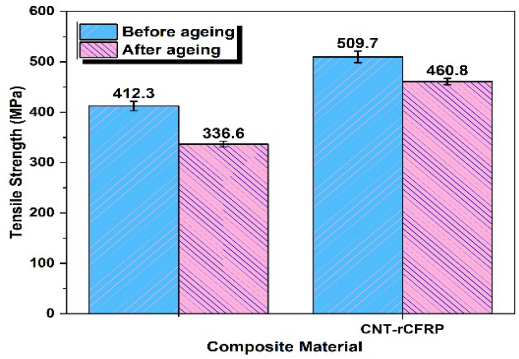


**Figure 8**: Tensile strength of rCFRP and CNT-rCFRP laminates before and after seawater hygrothermal ageing.

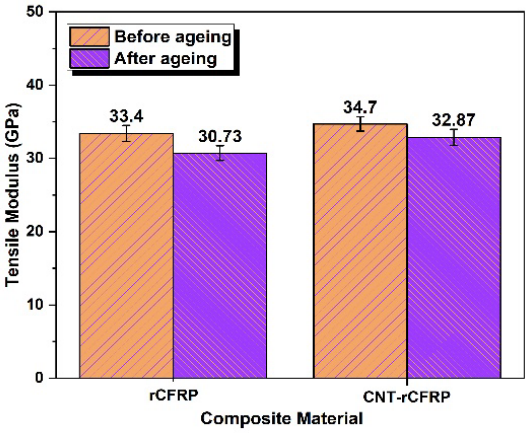


**Figure 9**: Tensile modulus of rCFRP and CNT-rCFRP laminates before and after seawater hygrothermal ageing.

After hygrothermal ageing, the corresponding values decreased to 336.6 and 460.8 MPa.

The rCFRP laminate retained 81.64% of its initial tensile strength, corresponding to a reduction of 18.36%. In comparison, CNT-rCFRP retained 90.41% of its initial tensile strength and showed a lower reduction of 9.59%. The absolute decreases in tensile strength were 75.7 MPa for rCFRP and 48.9 MPa for CNT-rCFRP. After ageing, the tensile strength of CNT-rCFRP remained 36.90% higher than that of rCFRP. A similar trend was observed for tensile modulus. The modulus of rCFRP decreased from 33.4 GPa before ageing to 30.73 GPa after ageing, while that of CNT-rCFRP decreased from 34.7 to 32.87 GPa. The retained tensile modulus was therefore 92.01% for rCFRP and 94.73% for CNT-rCFRP. The corresponding reductions were 7.99% and 5.27%, respectively.

The reduction in tensile properties after ageing can be attributed to moisture-induced plasticization of the epoxy matrix and weakening of the fiber–matrix interface. Moisture penetration can also promote swelling, interfacial debonding and microcrack formation, thereby reducing the efficiency of stress transfer between the matrix and the recycled carbon fibers.

The smaller decrease observed in CNT-rCFRP indicates that the CNT-modified interphase remained more stable during seawater exposure. The CNT network increased the interfacial contact area and improved mechanical interlocking between the recycled carbon fibers and the epoxy matrix. It also restricted moisture transport through interfacial gaps and defects. Consequently, CNT-rCFRP preserved a larger proportion of its tensile strength and modulus after hygrothermal ageing.

### *3.3 Impact properties of the composites before and after hygrothermal ageing*

The Izod impact test setup and the fractured specimens are shown in Figure 10. The Izod impact strengths of the rCFRP and CNT-rCFRP laminates before and after seawater hygrothermal ageing are compared in Figure 11. Before ageing, rCFRP and CNT-rCFRP exhibited impact strengths of 132.58 and 166.50 kJ/m², respectively. After ageing, the corresponding impact strengths decreased to 56.79 and 116.19 kJ/m².

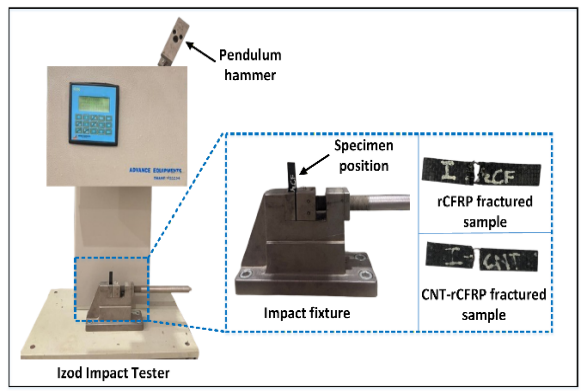


**Figure 10**: Izod impact test setup and fractured rCFRP and CNT-rCFRP specimens after hygrothermal ageing.

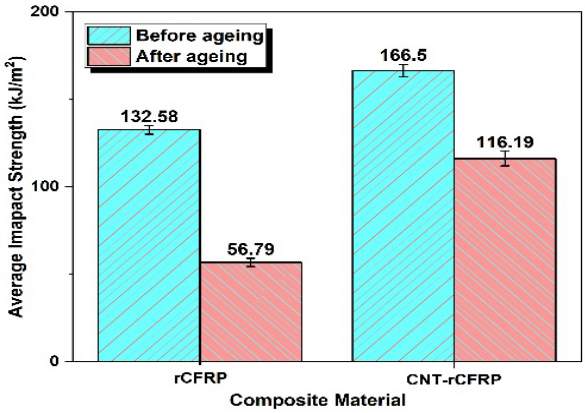


**Figure 11**: Izod impact strength of rCFRP and CNT-rCFRP laminates before and after seawater hygrothermal ageing.

The rCFRP laminate retained 42.83% of its initial impact strength and showed a reduction of 57.17%. In comparison, CNT-rCFRP retained 69.78% of its initial impact strength, corresponding to a smaller reduction of 30.22%. The absolute decreases in impact strength were 75.79 kJ/m² for rCFRP and 50.31 kJ/m² for CNT-rCFRP. Under the aged condition, the impact strength of CNT-rCFRP was 104.59% higher than that of rCFRP.

The greater loss in the impact strength of rCFRP can be associated with moisture-induced softening of the epoxy matrix and degradation of the recycled fiber–matrix interface. These weakened regions provided easier paths for crack initiation and propagation during sudden loading, thereby reducing the energy absorbed before fracture.

In CNT-rCFRP, the CNT-rich interphase improved fiber-matrix adhesion and restricted interfacial damage during ageing. During impact loading, the CNT network also promoted crack deflection, crack bridging, matrix fragmentation and resistance to fiber pull-out. These mechanisms increased the energy required for crack propagation and enabled CNT-rCFRP to retain a larger proportion of its initial impact strength.

### *3.4 SEM fractography and interphase-controlled damage mechanisms*

SEM fractography was carried out to identify the failure mechanisms responsible for the different impact responses of the aged rCFRP and CNT-rCFRP laminates. The fracture surfaces are shown in Figure 12, while the proposed damage mechanism is schematically illustrated in Figure 13.

The aged rCFRP laminate showed relatively clean recycled carbon fibers, fiber pull-out, interfacial debonding, and matrix-shear regions. These features indicate weak adhesion between the recycled carbon fibers and the epoxy matrix after seawater ageing. Moisture ingress can plasticize the epoxy and weaken the fiber/matrix interface, allowing cracks to propagate easily along the interfacial region. Because of this, the laminate fails due to fiber debonding and matrix deformation, which is why it has a lower impact strength.

In contrast, the CNT-rCFRP laminate showed a rougher and more irregular fracture surface. CNT-rich epoxy was observed to remain attached to the fiber surface, indicating stronger fiber/matrix bonding. The presence of fragmented matrix regions, broken fibers, and pulled-out CNTs suggests that the CNT-modified interphase resisted crack propagation more effectively.

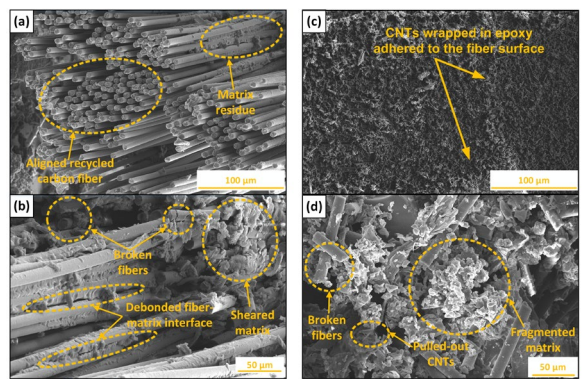


**Figure 12**: SEM fractographs of aged laminates: (a,b) rCFRP; (c,d) CNT-rCFRP.

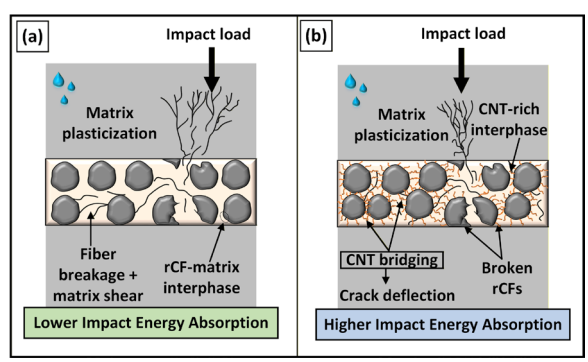


**Figure 13**: Schematic of impact-damage mechanisms in aged (a) rCFRP and (b) CNT-rCFRP laminates.

Instead of allowing cracks to travel directly through the interface, the CNT-rich region promoted crack deflection, crack bridging, and local matrix tearing.

These fracture features support the impact results discussed in Section 3.3. The rCFRP laminate absorbed less impact energy because damage was mainly concentrated along the weakened fiber/matrix interface. In the CNT-rCFRP laminate, the CNT-rich interphase increased the fracture resistance by forcing the crack to follow a more tortuous path. This increased the effective fracture surface area and required additional energy for matrix shearing, fiber breakage, CNT pull-out, and interfacial separation.

The damage sequence proposed in Figure 13 explains the difference between the two laminates. In the rCFRP laminate, seawater ageing softens the epoxy matrix and weakens the fiber/matrix interface. Under impact loading, cracks move quickly through these weakened regions, so the rCFRP laminate absorbs less energy before failure. In the CNT-rCFRP laminate, the CNT-rich interphase offers stronger resistance to crack growth. It bridges the crack, redirects its path, and improves load transfer across the damaged area. This leads to a more distributed fracture process and allows the laminate to absorb more impact energy.

The SEM observations support this damage mechanism. The rCFRP laminate mostly failed by interfacial debonding and fiber pull-out. In contrast, the CNT-rCFRP laminate showed a rougher fracture surface, with fragmented matrix, broken fibers, CNT pull-out, and crack-bridging features. These features indicate that CNT modification changed the fracture behaviour from interface-dominated failure to a tougher damage process with higher energy dissipation.

## 4. Conclusions

This study investigated the effect of CNT modification on the seawater hygrothermal ageing behaviour of recycled CFRP laminates. The CNT-rCFRP laminate showed lower moisture uptake than the unmodified rCFRP laminate. The equilibrium moisture uptake decreased from 1.20 to 0.72 wt.%, while the apparent diffusion coefficient decreased from $3.09 \times 10^{-13}$ to $2.31 \times 10^{-13}$ m²/s. These results indicate that the CNT-rich interphase restricted seawater transport through the laminate. Hygrothermal ageing reduced the tensile strength of rCFRP from 412.3 to 336.6 MPa and that of CNT-rCFRP from 509.7 to 460.8 MPa. The corresponding tensile-strength retentions were 81.64% and 90.41%, respectively. The tensile modulus decreased from 33.4 to 30.73 GPa for rCFRP and from 34.7 to 32.87 GPa for CNT-rCFRP, corresponding to modulus retentions of 92.01% and 94.73%, respectively. Similarly, the impact strength decreased from 132.58 to 56.79 kJ/m² for rCFRP and from 166.50 to 116.19 kJ/m² for CNT-rCFRP. CNT-rCFRP retained 69.78% of its initial impact strength, compared with 42.83% for rCFRP. Under the aged condition, the impact strength of CNT-rCFRP remained 104.59% higher than that of rCFRP. SEM fractography confirmed the difference in failure behaviour between the two laminates. The aged rCFRP laminate showed fiber pull-out, interfacial debonding and limited matrix deformation, indicating weak fiber–matrix adhesion. In contrast, CNT-rCFRP exhibited CNT-rich epoxy attachment, rough fracture surfaces, matrix fragmentation, fiber breakage and crack-bridging features. These observations indicate stronger interfacial bonding and a more distributed energy-dissipation process. Overall, CNT modification reduced moisture ingress and limited the deterioration of tensile and impact properties during seawater hygrothermal ageing, thereby improving the long-term durability of recycled CFRP laminates. Future work will focus on fatigue, interlaminar and thermomechanical properties of the composites.

## Author Contributions

A.S: investigation, methodology, writing an original draft; S.Z.: conceptualization, investigation, reviewing and editing. All authors have read and agreed to the published version of the manuscript.

## Conflicts of Interest

The authors declare no conflict of interest.

## Declaration of generative AI and AI-assisted technologies in the writing process

The authors used ChatGPT only for improvements in readability. The images, scientific content, analysis, mechanisms, interpretation, and conclusions were developed and verified entirely by the authors.

## References

[1] M. Pawlik, H. Le, and Y. Lu, “Effects of the graphene nanoplatelets reinforced interphase on mechanical properties of carbon fiber reinforced polymer – A

multiscale modelling study," *Composites Part B: Engineering*, vol. 177, Art. no. 107097, Nov. 2019, doi: 10.1016/j.compositesb.2019.107097.

[2] L. Bao, Y. Sun, F. Ruan, Y. Murakami, and Y. Yu, "Development of a method for recycling factory waste carbon fiber prepregs and increasing the added value of the collected material," *Polymer Composites*, vol. 44, no. 4, pp. 2071–2079, Apr. 2023, doi: 10.1002/pc.27244.

[3] K. Kawajiri and K. Sakamoto, "Environmental impact of carbon fibers fabricated by an innovative manufacturing process on life cycle greenhouse gas emissions," *Sustainable Materials and Technologies*, vol. 31, Art. no. e00365, Apr. 2022, doi: 10.1016/j.susmat.2021.e00365.

[4] S. Olhan, B. Antil, and B. K. Behera, "Repair technologies for structural polymeric composites: An automotive perspective," *Composite Structures*, vol. 352, Art. no. 118711, Jan. 2025, doi: 10.1016/j.compstruct.2024.118711.

[5] S. Pimenta and S. T. Pinho, "Recycling carbon fiber reinforced polymers for structural applications: Technology review and market outlook," *Waste Management*, vol. 31, no. 2, pp. 378–392, Feb. 2011, doi: 10.1016/j.wasman.2010.09.019.

[6] G. Oliveux, L. O. Dandy, and G. A. Leeke, "Current status of recycling of fiber reinforced polymers: Review of technologies, reuse and resulting properties," *Progress in Materials Science*, vol. 72, pp. 61–99, Jul. 2015, doi: 10.1016/j.pmatsci.2015.01.004.

[7] A. Sharma and S. Zafar, "Enhancing multifunctional properties of recycled carbon fiber composites through graphene nanoplatelet integration," *Polymer Composites*, pp. 1–13, Aug. 2025, doi: 10.1002/pc.70257.

[8] H. Li *et al.*, "The road ahead in interfacial engineering of recycled fiber composites," *Composites Part B: Engineering*, vol. 317, Art. no. 113613, Mar. 2026, doi: 10.1016/j.compositesb.2026.113613.

[9] J. Deng *et al.*, "Recycling of carbon fibers from CFRP waste by microwave thermolysis," *Processes*, vol. 7, no. 4, Art. no. 207, Apr. 2019, doi: 10.3390/pr7040207.

[10] O. Zabihi, M. Ahmadi, C. Liu, R. Mahmoodi, Q. Li, and M. Naebe, "Development of a low cost and green microwave assisted approach towards the circular carbon fiber composites," *Composites Part B: Engineering*, vol. 184, Art. no. 107750, Mar. 2020, doi: 10.1016/j.compositesb.2020.107750.

[11] Z. Deng, J. Fan, Z. Huang, and X. Yang, "Efficient recycling of carbon fiber from carbon fiber reinforced composite and reuse as high performance electromagnetic shielding materials with superior mechanical strength," *Polymer Testing*, vol. 125, Art. no. 108110, Aug. 2023, doi: 10.1016/j.polymertesting.2023.108110.

[12] E. Lester, S. Kingman, K. H. Wong, C. Rudd, S. Pickering, and N. Hilal, "Microwave heating as a means for carbon fiber recovery from polymer composites: A technical feasibility study," *Materials Research Bulletin*, vol. 39, no. 10, pp. 1549–1556, Aug. 2004, doi: 10.1016/j.materresbull.2004.04.031.

[13] M. S. Ansari, S. Zafar, and H. Pathak, "Upcycling CFRP waste for aerospace applications: Recovery of carbon fibers, CNT growth, and composite fabrication," *Polymer Composites*, vol. 46, no. S1, pp. S142–S158, Mar. 2025, doi: 10.1002/pc.29771.

[14] R. Kumar and S. Zafar, "Comparative study of microwave and thermal curing processes in terms of temperature characteristics and mechanical performance of carbon fibre composites," *Proceedings of the Institution of Mechanical Engineers, Part E: Journal of Process Mechanical Engineering*, vol. 238, no. 6, pp. 2728–2739, Dec. 2024, doi: 10.1177/09544089231162778.

[15] M. Rani, P. Choudhary, V. Krishnan, and S. Zafar, "A review on recycling and reuse methods for carbon fiber/glass fiber composites waste from wind turbine blades," *Composites Part B: Engineering*, vol. 215, Art. no. 108768, Jun. 2021, doi: 10.1016/j.compositesb.2021.108768.

[16] S. J. Pickering, "Recycling technologies for thermoset composite materials-current status," *Composites Part A: Applied Science and Manufacturing*, vol. 37, no. 8, pp. 1206–1215, Aug. 2006, doi: 10.1016/j.compositesa.2005.05.030.

[17] A. K. Gupta, R. Kiran, S. Zafar, and H. Pathak, "Effect of hygrothermal ageing on the mechanical properties of glass fiber reinforced polymer composite: Experimental and numerical approaches," *Materials Today Communications*,

vol. 41, Art. no. 111060, Dec. 2024, doi: 10.1016/j.mtcomm.2024.111060.

[18] C. Li, L. Zhang, H. Wang, Y. Song, and J. Wang, "Study of hygrothermal aging for basalt fiber/epoxy resin composites modified with CeCl3," *Polymers*, vol. 16, no. 6, Art. no. 819, Mar. 2024, doi: 10.3390/polym16060819.

[19] A. Salas *et al.*, "Ultrafast carbon nanotubes growth on recycled carbon fibers and their evaluation on interfacial shear strength in reinforced composites," *Scientific Reports*, vol. 11, no. 1, Art. no. 5000, Mar. 2021, doi: 10.1038/s41598-021-84419-y.

[20] R. Sahu, S. A. Ponnusami, C. Weimer, and D. Harursampath, "Interface engineering of carbon fiber composites using CNT: A review," *Polymer Composites*, vol. 45, no. 1, pp. 9–42, Jan. 2024, doi: 10.1002/pc.27772.

[21] R. Das *et al.*, "MWCNTs modified epoxy composites reinforced with kapok fiber: Mechanical and vibrational study for automotive applications," *Polymer Composites*, vol. 47, no. 6, pp. 5255–5270, Jun. 2026, doi: 10.1002/pc.70487.

[22] Q. Li, J. S. Church, M. Naebe, and B. L. Fox, "Interfacial characterization and reinforcing mechanism of novel carbon nanotube – Carbon fiber hybrid composites," *Carbon*, vol. 109, pp. 74–86, Nov. 2016, doi: 10.1016/j.carbon.2016.07.058.

[23] M. S. Ansari, S. Zafar, and H. Pathak, "Effect of stepped microwave irradiation to develop carbon nanotubes on carbon fiber for enhanced performance," *Vacuum*, vol. 218, Art. no. 112666, Dec. 2023, doi: 10.1016/j.vacuum.2023.112666.

[24] C. Nwambu, C. Robert, and P. Alam, "Tensile behaviour of unaged and hygrothermally aged discontinuous Bouligand structured CFRP composites," *Oxford Open Materials Science*, vol. 3, no. 1, Art. no. itac016, Jan. 2023, doi: 10.1093/oxfmat/itac016.

[25] A. K. Gupta, S. Zafar, and H. Pathak, "Mechanical durability of marine-grade glass fiber-reinforced polymer composites exposed to accelerated hygrothermal aging in seawater," *Journal of Composite Materials*, vol. 60, no. 18, pp. 1665–1680, Oct. 2025, doi: 10.1177/00219983251391882.

[26] M. Rani and S. Zafar, "Mechanical performance of glass fibers reinforced polymer composites obtained from microwave assisted chemical recycling," *Journal of Reinforced Plastics and Composites*, vol. 45, no. 7–8, pp. 1562–1579, Apr. 2026, doi: 10.1177/07316844251331997.